

Enhanced electrical conductivity of polyaniline films by postsynthetic DC high-voltage electrical field treatment

Lenka Kulhánková^a, Jonáš Tokarský^{a*}, Lubomír Ivánek^b, Veleoslav Mach^b, Pavlína Peikertová^a, Vlastimil Matějka^a, Kateřina Mamulová Kutláková^a, Jindřich Matoušek^c, Pavla Čapková^c

^a Nanotechnology Centre, VŠB-Technical University of Ostrava, 17. listopadu 15/2172, 708 33 Ostrava-Poruba, Czech Republic.

^b Faculty of Electrical Engineering and Computer Science, VŠB-Technical University of Ostrava, 17. listopadu 15/2172, 708 33 Ostrava-Poruba, Czech Republic.

^c Faculty of Science, University of J.E.Purkyně, České mládeže 8, 400 96 Ústí nad Labem, Czech Republic.

Abstract

New approach of chemical bath deposition combined with drying of freshly polymerized PANI films in high voltage (HV) static electrical field 0.6 – 2.7 kV/cm has been applied in present work. AFM and SEM microscopy revealed the significant changes of structure and morphology of PANI films, however the most important result of HV treatment was the strong increase of conductivity of PANI films from 88 S/m for the reference sample untreated in HV field up to 374 S/m for samples dried in the electric field (1.0 kV/cm). The dependence of PANI conductivity on the intensity of HV field showed the maximum conductivity for 1.0 kV/cm. Effects of corona discharge observed for HV field intensity above 2.0 kV/cm on the samples are also presented. Results showed the possibility to change the nanostructure and morphology using HV electrical field.

Keywords: high-voltage; polyaniline; thin film; conductivity; morphology

* Corresponding author, Tel.: +420 597 321 519, Fax.: +420 597 321 640

Address: Nanotechnology Centre, VŠB – Technical University of Ostrava, 17. listopadu 15, 70833 Ostrava, Czech Republic.

E-mail address: jonas.tokarsky@vsb.cz

1. Introduction

Polyaniline (PANI) is very interesting conducting polymer offering unusual electrical and optical properties together with environmental stability and good redox reversibility [1,2]. Taking into account the wide availability and low cost of aniline and its derivatives, PANI is an ideal candidate in various applications such as electrochromic devices [3,4], light-emitting diodes [5], gas and pH sensing [6-9], or corrosion protection [10,11]. Thin film is very frequently studied form of PANI and various substrates for PANI thin film deposition can be found in literature: zinc selenide [12], gold [13], polyvinyl chloride [14], quartz [15], glass and many others. For more information the reader is referred to the review published by Stejskal et al. [16]. The coating of glass substrate with PANI thin film has been achieved by various preparation methods [8,9,17-21]. The average conductivity of PANI thin films polymerized in water and deposited on glass substrate is reported by Stejskal et al. to be 260 ± 70 S/m [22]. Present study shows the possibility to modify conductivity of PANI thin films by treatment in high-voltage field in the range 0.6 – 2.7 kV/cm. Prepared samples were compared with reference sample (untreated by high-voltage field) in order to estimate the influence of this treatment on morphology and optical/electrical properties.

2. Experimental details

2.1. Preparation of PANI thin films

Aniline, sulfuric acid, and ammonium peroxydisulfate were purchased from Lach-Ner, Czech Republic, and used as received. The glass slides (76 mm × 26 mm × 1 mm) were washed in a soap solution, rinsed with distilled water, then with ethanol and dried. In order to prevent the two-sided coating of glass slides with PANI film, one side of the glass slides was covered by a scotch tape. PANI films on such treated glass slides were prepared using two solutions (0.2 M aniline prepared in 0.5 M sulfuric acid and 0.1 M ammonium peroxydisulfate dissolved in distilled water) mixed together.

Glass slides attached by clips and hanging on strings were introduced into the beaker before the polymerization and formation of thin film start. After 20 minutes, glass slides with PANI film were removed from the beaker and rinsed with 0.2 M hydrochloric acid. Prepared samples were dried in the DC high-voltage (HV) field. DC voltage source MBS 601 (Tesla Brno) allowing the regulation of the voltage in the range 0 - 10 kV was used. Scheme of the

apparatus for generating the HV field is shown in Fig. 1. The intensities used were 0.6, 1.0, 1.5, 2.0, 2.7 kV/cm and prepared samples were denoted as P_0.6, P_1.0, P_1.5, P_2.0, and P_2.7, respectively. Reference sample (denoted as P_0) has been prepared under the same conditions and let dried out of the field.

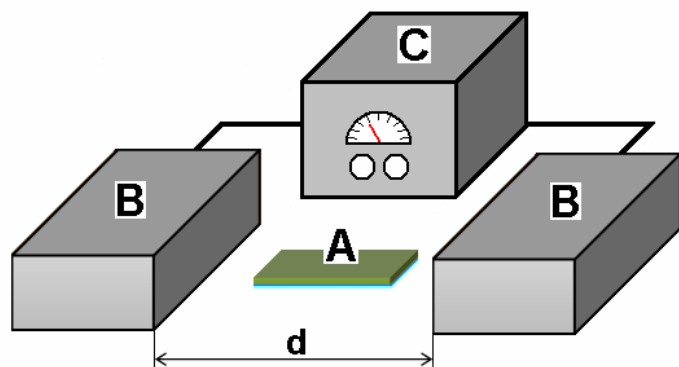


Fig. 1. Scheme of the apparatus for generating the high voltage field. Sample (A) is situated between two adjustable electrodes (B) powered from DC voltage source (C). Intensity value is determined by the applied voltage and distance d between electrodes.

2.2. Samples characterization

The morphology of the surfaces of thin PANI films was studied using atomic force microscopy and scanning electron microscopy. SolverNEXT (NT-MDT) atomic force microscope (AFM) equipped with contact probe PPP-CONTR (Nanosensors) was used for imaging. The images were evaluated using IA P9 software (NT-MDT). Images from the measurement on QUANTA 450 FEG (FEI) scanning electron microscope (SEM) were obtained using a secondary electron detector. Accelerating voltage used was 15 kV.

Conductivity of the samples has been measured by static applied voltage in DC regime using electrodes made of conductive rubber (Fig. 2). Following instruments were used: DC POWER SUPPLY HY 3003 D-2, V-meter UNI-T UT802, pA-meter KEITHLEY 6487. This special apparatus has been developed in order to eliminate the effect of structural inhomogeneity on the conductivity of PANI films. The value of DC voltage was 2V. The measured section (distance between electrodes \times width of the glass slide, see Fig. 2) was in the middle of thin PANI film (length 26 mm). The design of the measuring apparatus guarantee the same distance between electrodes, i.e. 5 mm (Fig. 2), as well as the perfect fit of electrodes and surface for all measurements. Contact force between the PANI film and electrodes was the same for all samples. During and after repeated measurements, there was no visible damage of the PANI thin films caused by the electric current flowing through the samples.

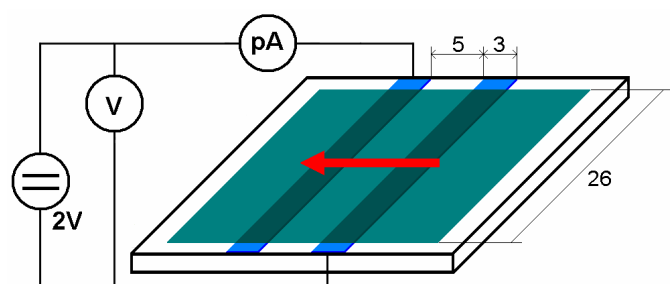


Fig. 2. Experimental apparatus for measuring the DC conductivity of PANI thin films. Sample (dark green) lies on the plexiglass base with two electrodes (blue) made of conductive rubber. Sizes and distances are provided in [mm]. Red arrow indicates the direction of HV field during the preparation process.

Smart Raman Microscopy System XploRATM (HORIBA Jobin Yvon, France) was used for study of PANI thin films. Raman spectra were acquired with 532 nm excitation laser source, with 100× objective and using 1200 gr./mm grating. UV-VIS spectra were registered using spectrophotometer CINTRA 303 (GBC Scientific Equipment). The optical transmittance was measured at normal incidence at room temperature in the spectral range of 800–350 nm. Speed was 1000 nm/min with step size 0.427 nm, slit width was 2.0 nm.

3. Results and discussion

3.1. Conductivity

Results of conductivity measurements in dependence on HV field intensity are summarized in Table 1 and displayed in Fig. 3a. It is evident that drying in HV field up to 1 kV/cm leads to significant increase of conductivity while further increase of HV field results in decrease of conductivity until the intensity 2 kV/cm is reached. For HV field intensity above 2 kV/cm the corona discharge has been observed and the conductivity of P_2.7 sample was found to be again very high.

Table 1. Main characteristics of all samples are listed in the following order: applied high-voltage field (HV); average thickness of thin PANI film (d_{av}); conductivity (σ); the most frequent height (h_{mf}) of PANI „stalagmites“; maximum transmittance with corresponding wavelength ($T_{max}(\lambda)$).

sample	HV (kV/cm)	d_{av} (nm)	σ (S/m)	h_{mf} (nm)	T_{max} [%] (λ [nm])
P_0	0.0	95	88	112.2	0.82 (532)
P_0.6	0.6	90	329	102.4	0.79 (515)
P_1.0	1.0	90	374	80.0	0.82 (522)
P_1.5	1.5	105	328	95.0	0.83 (520)
P_2.0	2.0	90	214	102.2	0.82 (513)
P_2.7	2.7	90	541	91.3	0.80 (519)

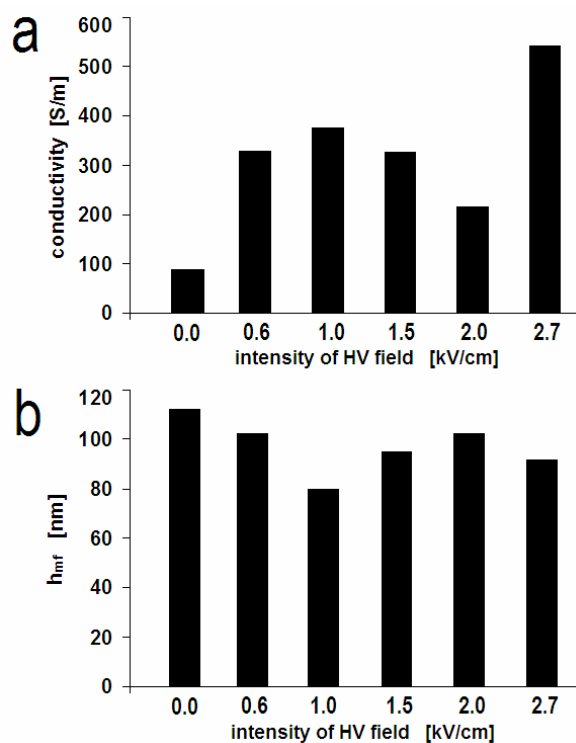


Fig. 3. Bar charts showing clearly the dependencies of (a) conductivity and (b) the most frequent height of PANI “stalagmites” (h_{mf}) on high-voltage field intensity.

3.2. Morphology changes

As one can see in Fig. 4, HV field influences the surface morphology of dried PANI thin films. The high „stalagmites“ observed on the surface of the reference sample P_0 are less frequent for samples dried in HV field. In order to describe the morphology changes quantitatively, frequency analysis of the PANI „stalagmites“ heights was performed and the results are shown in Fig. 5.

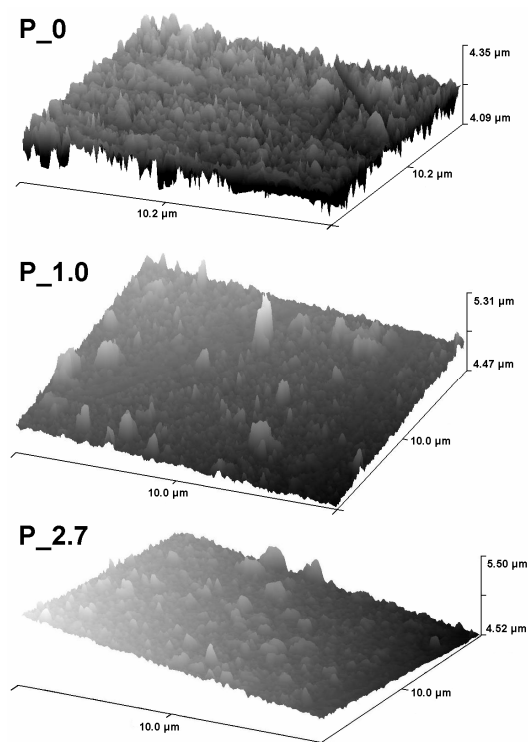


Fig. 4. AFM images of samples P_0, P_1.0 and P_2.7 show the differences in morphology of PANI thin films.

Special attention has been paid to the maximum of “stalagmites” height distribution (h_{mf}) for samples treated in different HV field intensity. The dependence of h_{mf} on HV field intensity is on the bar chart in Fig. 3b and the h_{mf} values are listed in the Table 1. The “stalagmites” height decreased in the range 0.0 – 1.0 kV/cm. The minimum “stalagmites” height corresponds to the highest conductivity (compare Figs. 3a and 3b). For higher HV field intensity up to 2.0 kV/cm the increase of “stalagmites” height was observed together with decrease of conductivity. At intensity higher than 2.0 kV/cm the corona discharge has been observed which resulted in violation of the opposite course of both dependencies σ/HV and h_{mf}/HV for intensity 2.7 kV/cm (Figs. 3a and 3b). Taking into account the interrelation between σ and h_{mf} for lower intensities, here the h_{mf} value is much higher than would be expected. Therefore, present results suggest that such high intensity can affect the PANI structure. In order to study the structural changes the Raman spectroscopy was involved and the spectra for all samples can be found in Fig. 6.

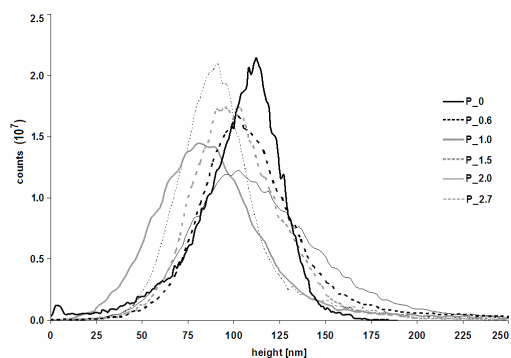


Fig. 5. Frequency analysis of heights of PANI „stalagmites“ for all samples.

At first sight, Raman spectra do not indicate distinct changes of molecular structures. That means the conductivity really depends mainly on the morphology and microstructure of PANI thin films as detected by AFM microscopy. However, this conclusion is not valid for the sample P_2.7 dried at 2.7 kV/cm for which the Raman spectrum exhibits variances in the range 1480-1650 cm^{-1} (see Fig. 6). These are characteristic for partially decomposed PANI as described in [23,24]. As this sample was in fact exposed by corona plasma treatment the different behaviour is understandable.

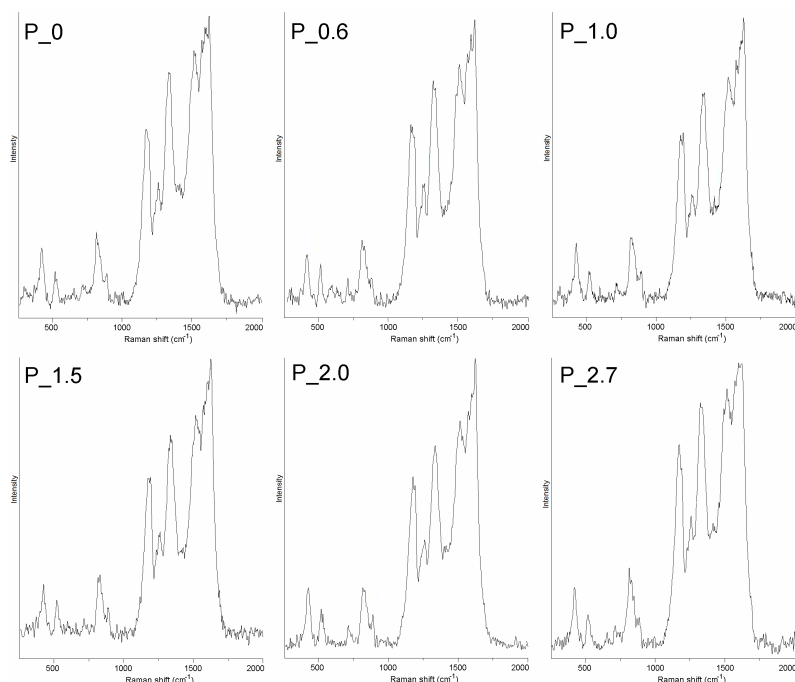


Fig.6. Raman spectra for all prepared samples.

Morphology of the samples was also characterized by SEM microscopy. Comparison of SEM images in Fig. 7 revealed the pronounced changes of microstructure and surface morphology in dependence on the HV field intensity. This observation agrees with AFM results. It can be

concluded that HV field applied during drying led to the finer structure (i.e. smaller “stalagmites” diameters). One can see that average “stalagmites” diameter for P_2.7 sample is nearly three times smaller than for reference sample P_0.

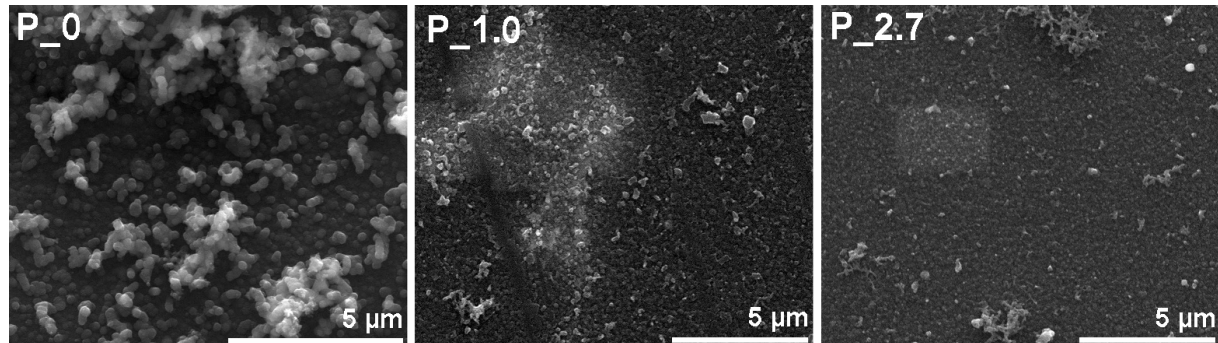


Fig. 7. SEM images of samples P_0, P_1.0 and P_2.7 show the differences in morphology of PANI thin films.

Optical transmittance in dependence on wavelength for all samples is shown in Fig. 8 and the maximum transmittance values with corresponding wavelengths are listed in Table 1. UV-VIS spectra follow the trend observed in our previous study, i.e. the lower transmittance the higher conductivity [25]. However, the range of values is very small and, therefore, the optical transmittances can be considered nearly the same.

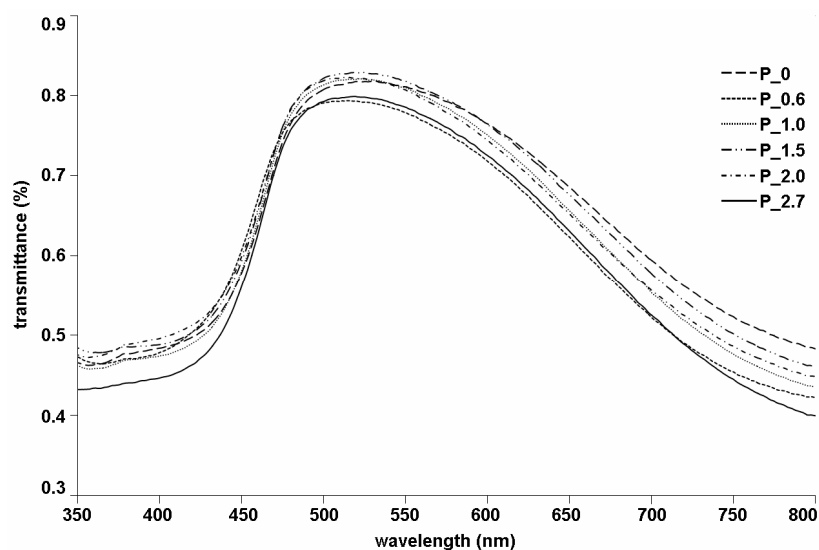


Fig. 8. UV-VIS spectra for all prepared samples.

4. Conclusions

Present results showed the chance to control the microstructure, morphology and conductivity of PANI films using drying wet freshly prepared PANI films in HV field. The HV field suppressed the growth of “stalagmites” and leads to more flat fine-grained surface and higher conductivity in the range 0.6-1.0 kV/cm. In general, the lower the „stalagmites“ height, the higher the conductivity. Further increase of HV field intensity up to 2.0 kV/cm led to slight increase of “stalagmites” heights and to decrease of conductivity. For the HV field with higher intensity the corona discharge appeared and samples undergo the plasma treatment accompanied with changes in polymer nanostructure and significant increase of conductivity associated, however, with a risk of polymer degradation. The optical transmittances of samples treated in HV field remain nearly the same as for the reference sample while the conductivities are significantly higher.

Acknowledgement

This research has been funded by the Grant Agency of Czech Republic (project P108/11/1057). Authors are grateful to Petra Vilímová for her indispensable technical help with AFM measurements.

References

- [1] I. Sapurina, J. Stejskal, The mechanism of the oxidative polymerization of aniline and the formation of supramolecular polyaniline structures, *Polym. Int.* 57 (2008) 1295-1325.
- [2] A.G. MacDiarmid, Synthetic metals: a novel role for organic polymers, *Synth. Met.* 125 (2002) 11-22.
- [3] C.D. Batich, H.A. Laitinen, H.C. Zhou, Chromatic changes in polyaniline films, *J. Electrochem. Soc.* 137 (1990) 883-885.
- [4] T. Kobayashi, N. Yonevama, H. Tamura, Oxidative degradation pathway of polyaniline film electrodes, *J. Electroanal. Chem.* 177 (1984) 281-291.
- [5] S. Karg, J.C. Scott, J.R. Salem, M. Angelopoulos, Increased brightness and lifetime of polymer light-emitting diodes with polyaniline anodes, *Synth. Met.* 80 (1996) 111-117.
- [6] J. Janata, M. Josowicz, J. Organic semiconductors in potentiometric gas sensors, *Solid State Electrochem.* 13 (2009) 41-49.

- [7] N.E. Agbor, J.P. Cresswell, M.C. Petty, A.P. Monkman, An optical gas sensor based on polyaniline Langmuir-Blodgett films, *Sens. Actuators, B* 41 (1997) 137-141.
- [8] N. Menegazzo, B. Herbert, S. Banerji, K.S. Booksh, Discourse on the utilization of polyaniline coatings for surface plasmon resonance sensing of ammonia vapor, *Talanta* 85 (2011) 1369-1375.
- [9] M.M. Ayad, N.A. Salahuddin, M.O. Alghaysh, R.M. Issa, Phosphoric acid and pH sensors based on polyaniline films, *Curr. Appl. Phys.* 10 (2010) 235-240.
- [10] G.S. Gonçalves, A.F. Baldissera, L.F. Rodrigues Jr., E.M.A. Martini, C.A. Ferreira, Alkyd coatings containing polyanilines for corrosion protection of mild steel, *Synth. Met.* 161 (2011) 313-323.
- [11] W.K. Lu, R.L. Elsenbaumer, B. Wessling, Corrosion protection of mild steel by coatings containing polyaniline, *Synth. Met.* 71 (1995) 2163-2166.
- [12] I. Šeděnková, M. Trchová, N.V. Blinova, J. Stejskal, In-situ polymerized polyaniline films. Preparation in solutions of hydrochloric, sulfuric, or phosphoric acid, *Thin Solid Films* 515 (2006) 1640-1646.
- [13] C.J. Liu, K. Hayashi, K. Toko, A novel formation process of polyaniline micro-/nanofiber network on solid substrates, *Synth. Met.* 159 (2009) 1077-1081.
- [14] T.V. Shishkanova, P. Matějka, V. Král, I. Šeděnková, M. Trchová, J. Stejskal, Optimization of the thickness of a conducting polymer, polyaniline, deposited on the surface of poly(vinyl chloride) membranes: A new way to improve their potentiometric response, *Anal. Chim. Acta* 624 (2008) 238-246.
- [15] M.M. Ayad, N.L. Torad, Alcohol vapours sensor based on thin polyaniline salt film and quartz crystal microbalance, *Talanta* 78 (2009) 1280-1285.
- [16] J. Stejskal, I. Sapurina, M. Trchova, Polyaniline nanostructures and the role of aniline oligomers in their formation, *Prog. Polym. Sci.* 35 (2010) 1420-1481.
- [17] Z.F. Li, E. Ruckenstein, Conductive surface via graft polymerization of aniline on a modified glass surface, *Synth. Met.* 129 (2002) 73-83.
- [18] N. Carrillo, U. León-Silva, T. Avalos, M.E. Nicho, S. Serna, F. Castillon, M. Farias, R. Cruz-Silva, Enzymatically synthesized polyaniline film deposition studied by simultaneous open circuit potential and electrochemical quartz crystal microbalance measurement, *J. Colloid Interface Sci.* 369 (2012) 103-110.
- [19] S.B. Kulkarni, S.S. Joshi, C.D. Lokhande, Facile and efficient route for preparation of nanostructured polyaniline thin films: Schematic model for simplest oxidative chemical polymerization, *Chem. Eng. J.* 166 (2011) 1179-1185.

- [20] M.M. Ayad, M.A. Shenashin, Film thickness studies for the chemically synthesized conducting polyaniline, *Eur. Polym. J.* 39 (2003) 1319-1324.
- [21] Y. Wang, X. Jing, Transparent conductive thin films based on polyaniline nanofibers, *Mater. Sci. Eng., B* 138 (2007) 95-100.
- [22] J. Stejskal, I. Sapurina, Polyaniline: Thin films and colloidal dispersions (IUPAC Technical Report), *Pure Appl. Chem.* 77 (2005) 815–826.
- [23] R. Mažeikiene, G. Niaura, A. Malinauskas, Raman spectroelectrochemical study on the kinetics of electrochemical degradation of polyaniline. *Polym. Degrad. Stab.* 93 (2008) 1742–1746.
- [24] I. Šeděnková, M. Trchová, J. Stejskal, Thermal degradation of polyaniline films prepared in solution of strong and weak acids in water – FTIR and Raman spectroscopic studies. *Polym. Degrad. Stab.* 93 (2008) 2147–2157.
- [25] J. Tokarský, L. Kulhánková, K. Mamulová Kutlákova, P. Peikertová, J. Svatuška, V. Stýskala, V. Matějka, V. Vašínek, P. Čapková, Monitoring the conductivity and optical homogeneity during the growth of PANI thin films. *Thin Solid Films* (2013) *accepted manuscript, not on-line yet.*